

Development of Novel Silicon Detectors at the MPI Semiconductor Laboratory

Gerhard Lutz
MPI-Semiconductor Laboratory, München
RAL, Sept. 12, 2003

1

Content

- Introduction
- Semiconductor properties
- Diode and strip detectors
- Detector fabrication -- The laboratory
- Drift detectors
 - for position measurement (tracking)
 - for energy measurement (spectroscopy)
- CCD detectors
 - pn-CCDs in X-ray astronomy
- DEPFET detector-amplifier structure
 - Principle and properties
 - As pixel detector
 - In x-ray astronomy (XEUS)
 - In particle colliders (TESLA)
- Detector thinning technology
- Summary and conclusions

G.Lutz, RAL, Sept.12, 2003

2

Introduction

- Activity in semiconductor detector since beginning (1979/80)
- Initiated by particle physics (strip detectors)
- Introduction of new detector concepts
- Extended to X-ray astronomy
- Culminating in the foundation of own Laboratory with complete semiconductor technology
- Supported by two Max-Planck institutes
- Development of novel detectors for institute experiments in astrophysics and particle physics

G.Lutz, RAL, Sept.12, 2003

3

Semiconductors as Nuclear Radiation Detectors

Outstanding Material Properties

- small band gap (Si 1.12eV) \Rightarrow low e-h pair generation energy (Si 3.6 eV) (ionisation energy for gases \gg 30 eV)
- High density (Si 2.33 g/cm³) \Rightarrow large energy loss/length for ionising particles \Rightarrow thin detectors; small range α -electrons; precise position measurement
- Almost free movement of electrons and holes
- Mechanical rigidity; self supporting structure, windowless operation
- Doping creates fixed space charges; building of sophisticated field structures
- integration of detector and electronics in single device

G.Lutz, RAL, Sept.12, 2003

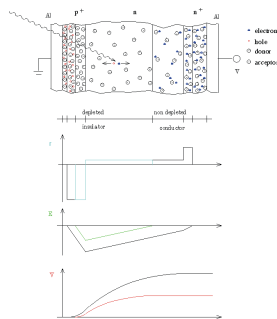
4

Basic Detector Structures

The Diode

Operation

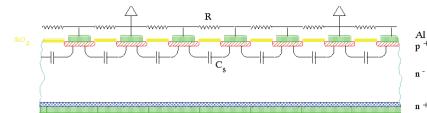
- unbiased: radiation level measurement only
- partially biased: single particle energy measurement
- biased above full depletion: fast and complete charge collection



G.Lutz, RAL, Sept.12, 2003

5

(Diode) Strip Detectors



Divide diode into strips and measure charge arriving at individual strips \Rightarrow position measurement

Further developments:

- charge division readout
- double sided readout
- capacitive coupled readout
- biasing methods
- breakdown protection
- radiation hardening

G.Lutz, RAL, Sept.12, 2003

6

Planar Technology

A "simple" production sequence:

Strip Detector

polished wafer type
oxidation
illumination mask
wafer coated with photoresist
photoresist development and etching
Boron and phosphorus implantation
Aluminium deposition
Aluminium structuring

G.Lutz, RAL Sept.12, 2003 7

MPI semiconductor laboratory

800 m² cleanroom up to class 1 ... with modern, custom made facilities ... for a full 6" silicon process line

mounting & bonding test & qualification simulation, layout & data analysis

Why own technology:

- Use of ultra-pure silicon:
- properties not to deteriorate during processing
- wafer size defect free processing
- double sided processing
- sophisticated detectors require complete and detailed control over process

G.Lutz, RAL Sept.12, 2003 9

(Historical) Detectors for particle physics

Particle tracking: position measurement

- First strip detectors (NA11/NA32)
- First double sided
- Capacitive coupled, simple biasing
- Radiation hard
- Pixel sensors
- (First drift detectors)
- Readout electronics

NA11 strip detector

Aleph strip detectors

G.Lutz, RAL Sept.12, 2003 10

Semiconductor Drift Chamber

Sideward depletion

Drift chamber (Gatti and Rehak 1984)

- Sideward depletion + graded potential on outer surface
- signal charge collected in centre valley, moves parallel to surface towards collecting anode
- drift time gives position
- small capacitive load gives good energy resolution

G.Lutz, RAL Sept.12, 2003

Semiconductor Detector

electronic noise

$$ENC^2 = A_1 \cdot 2qI_{leak} \cdot t + A_2 \cdot C_{tot}^2 H_{V/f} + A_3 \cdot C_{tot}^2 2kT \frac{a}{\delta_m} \frac{1}{t}$$

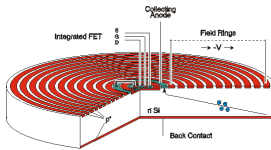
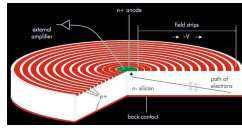
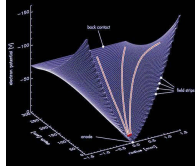
- leakage current
- low frequency noise
- thermal noise

12

Semiconductor Detectors for Spectroscopy

Drift Diode (Kenner+Lutz, 1987)

- Single sided structured
- Point anode \Rightarrow small capacitance, small electronic noise
- Thin, homogeneous radiation entrance window



Integration of first amplification

- Further improvement of noise performance

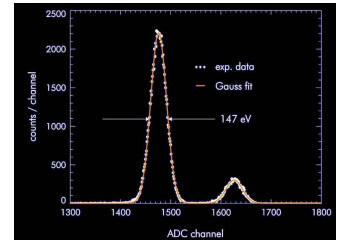
G.Lutz, RAL Sept.12, 2003

13

SDD performance

typical performance (10 mm², -10 °C)

- energy resolution
147 eV FWHM @ 5.9 keV
- peak-to-background
> 3.000
- thin entrance window
q.e. > 80 % (250 eV ... 12 keV)
- count rate capability
1.000.000 cps

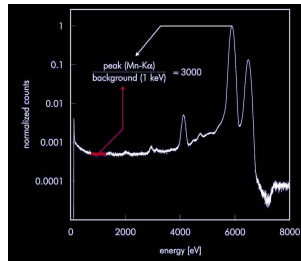


14

SDD performance

typical performance (10 mm², -10 °C)

- energy resolution
147 eV FWHM @ 5.9 keV
- peak-to-background
> 3.000
- thin entrance window
q.e. > 80 % (250 eV ... 12 keV)
- count rate capability
1.000.000 cps

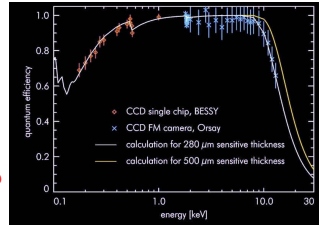


15

SDD performance

typical performance (10 mm², -10 °C)

- energy resolution
147 eV FWHM @ 5.9 keV
- peak-to-background
> 3.000
- thin entrance window
q.e. > 80 % (250 eV ... 12 keV)
- count rate capability
1.000.000 cps

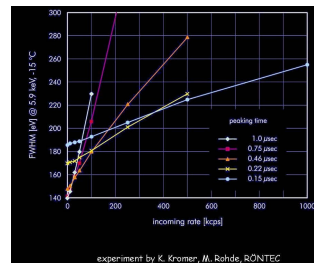


16

SDD performance

typical performance (10 mm², -10 °C)

- energy resolution
147 eV FWHM @ 5.9 keV
- peak-to-background
> 3.000
- thin entrance window
q.e. > 80 % (250 eV ... 12 keV)
- count rate capability
1.000.000 cps



experiment by K. Kromer, M. Rohde, RONTEC

SDD vs. other spectroscopy systems

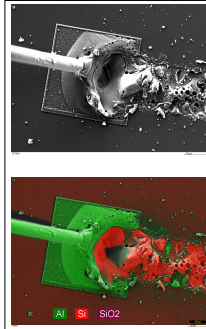
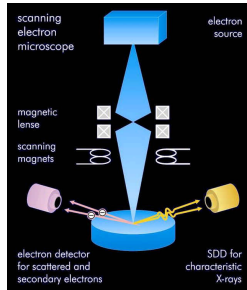
detector type	cooling method	thickness [mm]	active area [mm ²]	max. throughput [kcps]
Si(Li)	liquid nitrogen	3 ... 5	10 ... 200	30 ... 50
HPGe	liquid nitrogen	3	10 ... 20	30 ... 50
SDD	thermoelectric	0.3 ... 0.5	5 ... 10	400

detector type	dead time vs. count rate			FWHM [eV] Mn-Kα vs. count rate			
	100 kcps	150 kcps	800 kcps	1 kcps	50 kcps	100 kcps	1 Mcps
Si(Li)	50 %	95 %	-	-129	-190	-	-
HPGe	50 %	95 %	-	-109	-175	-	-
SDD	5 %	10 %	50 %	-145	-160	-215	-260

18

SDD - applications

electron microprobe analysis



figures by RÖNTEC

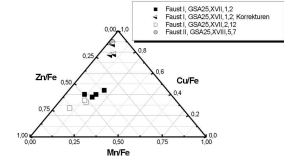
19

SDD - applications

X-ray fluorescence analysis, studies of art & archeological objects



J. W. v. Goethe, Faust I
original manuscript



"fingerprint" of Goethe's ink
⇒ editing of Faust I during Faust II work

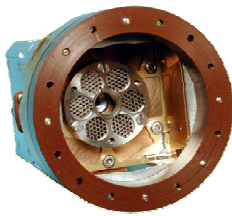
experiment & figures by O. Hahn (BAM, Berlin)

with portable system "artTAX" (RÖNTEC)

20

SDD - applications

particle induced X-ray emission



APXS

alpha-proton-X-ray spectrometer

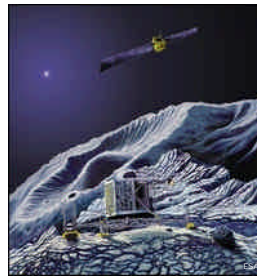
- ESA mission ROSETTA
comet orbiter & lander
67P/Churyumov-Gerasimenko
- NASA missions
2003 Mars Exploration Rover I + II

APXS systems by J. Brückner, R. Rieder
(MPI für Chemie, Kosmochemie, Mainz)

21

SDD - applications

particle induced X-ray emission



APXS

alpha-proton-X-ray spectrometer

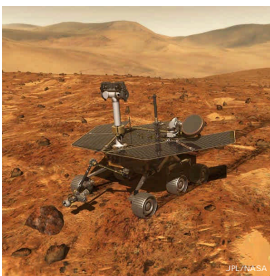
- ESA mission ROSETTA
comet orbiter & lander
67P/Churyumov-Gerasimenko
- NASA missions
2003 Mars Exploration Rover I + II

APXS systems by J. Brückner, R. Rieder
(MPI für Chemie, Kosmochemie, Mainz)

22

SDD - applications

particle induced X-ray emission



APXS

alpha-proton-X-ray spectrometer

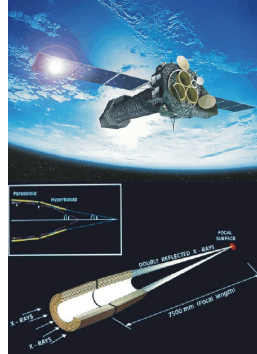
- ESA mission ROSETTA
comet orbiter & lander
67P/Churyumov-Gerasimenko
- NASA missions
2003 Mars Exploration Rover I + II

APXS systems by J. Brückner, R. Rieder
(MPI für Chemie, Kosmochemie, Mainz)

23

Detectors for X-ray astronomy

pn-CCD for ESA's XMM-Newton satellite

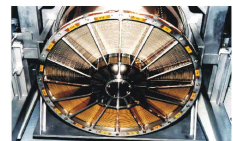


XMM: three X-ray telescopes

- one dedicated to imaging (with pn-CCD)
- two with additional reflecting gratings (and MOS CCDs)
- one optical telescope
- all pointing on same object

Wolter I type mirror telescopes

- 58 nested mirror shells
- Wall thickness 0.5 to 1mm Ni



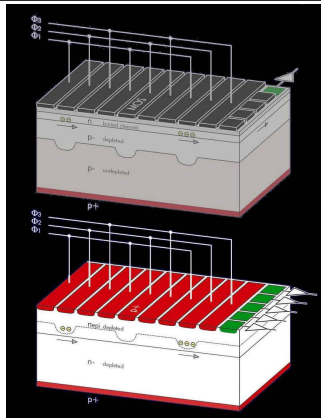
24

pn-CCD principle

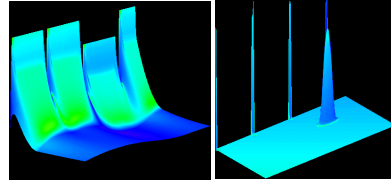
MOS-CCD (video CCD)

- MOS transfer gates
- implanted pn-junctions
- buried channel
- deep transfer
- partial depletion
- full depletion
- frontside illumination
- back entrance window
- serial readout
- 1 preamp / channel

pn-CCD



CCD device simulation

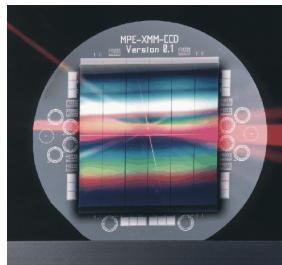


G.Lutz, RAL Sept.12, 2003

26

pn-CCD performance

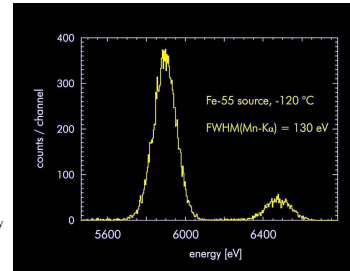
- largest monolithic CCD
- 6 x 6 cm²
- 384 x 400 pixel
- 150 μm pixel
- fast, parallel readout
- 5 msec full frame
- low noise
- 4 el. ms
- high quantum efficiency
- 90 %
- radiation hard
- 400 Mp/cm²



27

pn-CCD performance

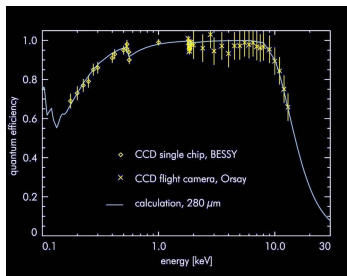
- largest monolithic CCD
- 6 x 6 cm²
- 384 x 400 pixel
- 150 μm pixel
- fast, parallel readout
- 5 msec full frame
- low noise
- 4 el. ms
- high quantum efficiency
- 90 %
- radiation hard
- 400 Mp/cm²



28

pn-CCD performance

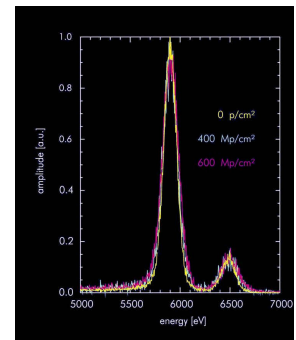
- largest monolithic CCD
- 6 x 6 cm²
- 384 x 400 pixel
- 150 μm pixel
- fast, parallel readout
- 5 msec full frame
- low noise
- 4 el. ms
- high quantum efficiency
- 90 %
- radiation hard
- 400 Mp/cm²



29

pn-CCD performance

- largest monolithic CCD
- 6 x 6 cm²
- 384 x 400 pixel
- 150 μm pixel
- fast, parallel readout
- 5 msec full frame
- low noise
- 4 el. ms
- high quantum efficiency
- 90 %
- radiation hard
- 400 Mp/cm²



30

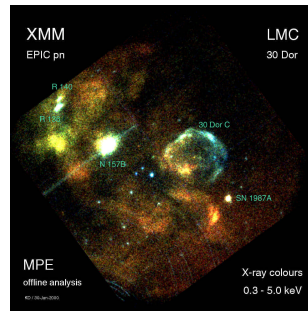
pn-CCD vs. MOS-CCD

	Type	energy resolution @ 272 eV & 5.9 keV FWHM [eV]		quantum efficiency @ 272 eV & 10 keV [%]		readout time [msec]	pixel cell size [μm^2]	detector size [cm^2]
CHANDRA (original)	MI T/LL-F1	60	130	3	20	500	24 x 24	2.5 x 2.5
	MI T/LL-B1	125	200	50	10	500	24 x 24	2.5 x 2.5
XMM	Leicester	80	130	25	30	500	40 x 40	2.4 x 2.4
	SRON	100	145	65	15	500	27 x 27	2.8 x 2.8
	pn-CCD	70	130	90	90	4,6	150 x 150	6 x 6

backside illumination
 full depletion
 large pixels, parallel readout

31

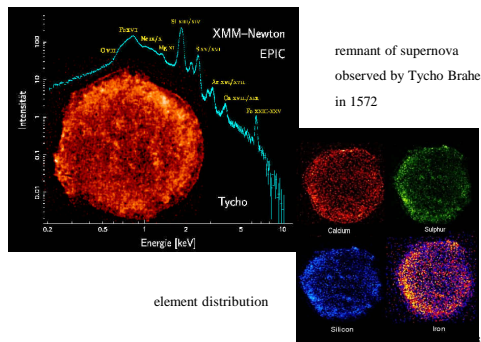
XMM-Newton – first light (January 2000)



large Magellanic cloud
 supernova remnant 1987A

32

XMM-Newton – observations

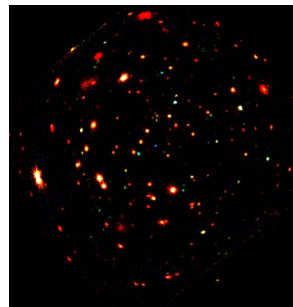


remnant of supernova observed by Tycho Brahe in 1572

element distribution

33

XMM-Newton – observations



Lockman hole:
 a look into deep space

first observation of 'green' and 'blue' hard x-ray sources

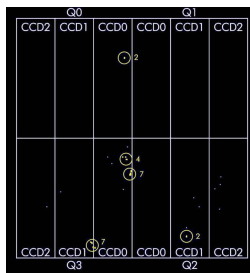
no diffuse background?

G.Lutz, RAL Sept.12, 2003

34

pn-CCD performance in space

- perfect imaging since launch
- detector performance equal to ground qualification
- no significant change of energy resolution and charge transfer efficiency
- few pixels lost in rev. 156 impact of micro-meteorite?
- effect reproduced on ground using a dust accelerator

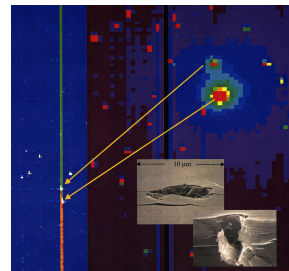


G.Lutz, RAL Sept.12, 2003

35

pn-CCD performance in space

- perfect imaging since launch
- detector performance equal to ground qualification
- no significant change of energy resolution and charge transfer efficiency
- few pixels lost in rev. 156 impact of micro-meteorite?
- effect reproduced on ground using a dust accelerator



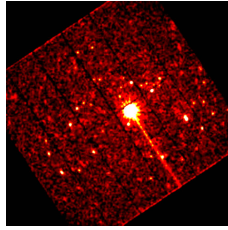
G.Lutz, RAL Sept.12, 2003

36

pn-CCD - limitation

charge transfer speed limited
by the time needed for readout

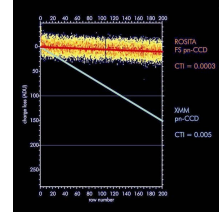
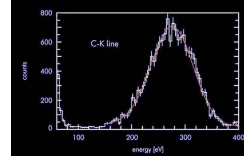
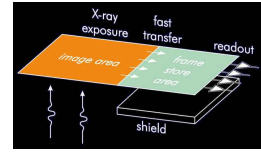
⇒ 'out of time' events
pn-CCD: ~ 6 %



37

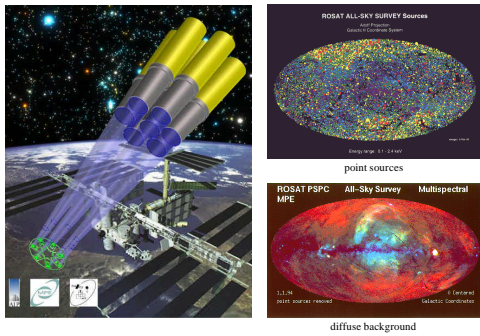
Frame Store pn-CCD

- frame store area
 - separation transfer / readout
 - reduction of out-of-time events
 - 6 % (XMM) → 0.4 %
- prototypes under test
 - smaller pixels (50 ... 75 μm)
 - larger format 128 x 128
 - improved performance



38

ROSITA - ROentgen Survey with an Imaging Telescope Array



G.Lutz, RAL, Sept.12, 2003

39

Pn-CCD works with low Clock voltage amplitude Dj

1486 eV (Al-K):

Dj = 8.0 V	CTI = 116 E-6	FWHM = 87 eV	← α-particle meas.
Dj = 2.0 V	CTI = 155 E-6	FWHM = 96 eV	
Dj = 1.5 V	CTI = 181 E-6	FWHM = 98 eV	
Dj = 1.3 V	CTI = 237 E-6	FWHM = 103 eV	(XMM: CTI = 660 E-6)

13.9 keV (Am²⁴¹ X-ray line) low gain mode:

Dj = 8.0 V	CTI = 83 E-6
Dj = 3.0 V	CTI = 96 E-6
Dj = 2.0 V	CTI = 179 E-6
Dj = 1.5 V	CTI = 200 E-6
Dj = 1.3 V	CTI = 265 E-6

(j = [-10 V; -25 V])

advantages of small Dj : - safety (lower electric field)
- faster clocking pulses
- less power dissipation

G.Lutz, RAL, Sept.12, 2003

40

Future X-ray Mission: XEUS (X-ray Evolving Universe Spectroscopy)

Scientific aim:
investigation of the universe at an early evolution stage:
- early black holes
- evolution and clustering of galaxies
- evolution of element synthesis

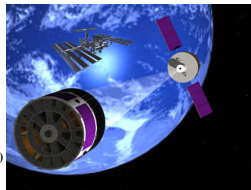
Experiment

- Increase in collecting area (factor 100)
- Increase of collection area (0.5 to 6-30m²)
- Increase in focal length (7.5 to 50m)
- Optics and focal imaging on separate satellites

Focal detector requirements:

- faster readout (factor 10 to 100)
- avoidance of "out of time" events
- larger size focal detector (7x7cm²)
- smaller pixel size (50-50μm²)

Detector requirements can be met with DEPFET pixel detectors

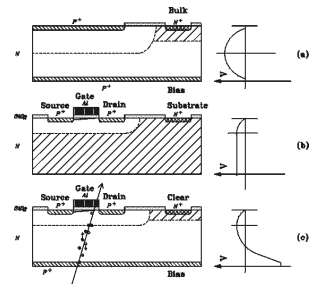


G.Lutz, RAL, Sept.12, 2003

41

The Depleted Field Effect Transistor (DEPFET)

- Device concept:**
- Combination of FET transistor with
 - Sideward depletion (Drift chamber)



G.Lutz, RAL, Sept.12, 2003

42

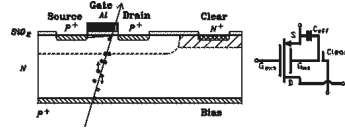
Operation principle of DEPFET

DEPFET structure and device symbol.

- Field effect transistor on top of fully depleted bulk
- All charge generated in fully depleted bulk
- assembles underneath the transistor channel
- steers the transistor current

Combined function of sensor and amplifier

- low capacitance and low noise
- Signal charge remains undisturbed by readout
- repeated readout for noise reduction
- Complete clearing of signal charge
- no reset noise
- Full sensitivity over whole bulk
- Thin radiation entrance window on backside

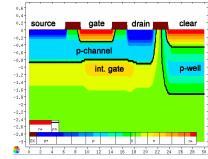


G.Lutz, RAL Sept.12, 2003

43

DEPFET types:

- > MOS-enhancement
- > MOS-depletion
- > JFET
- ◇ Open (rectangular) geometry
- ◇ Closed (circular) geometry



DEPFET applications

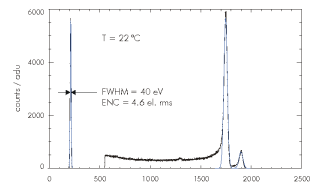
- Readout element of
 - > Drift detector
 - > CCD
- Element of pixel detector

G.Lutz, RAL Sept.12, 2003

44

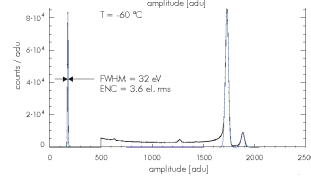
DEPFET ⁵⁵Fe Spectrum

Single DEPFET (JFET, closed geometry)



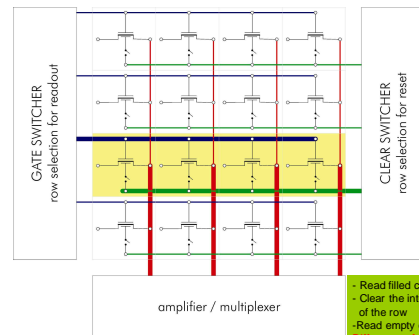
At room temperature

Cooled



G.Lutz, RAL Sept.12, 2003

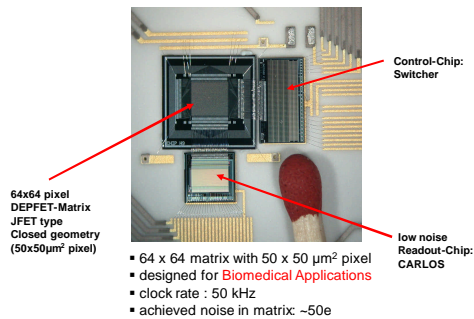
DEPFET pixel matrix



- Read filled cells of a row
- Clear the internal gates of the row
- Read empty cells
- Difference of readings (filled/empty) measures charge

G.Lutz, RAL Sept.12, 2003

Prototype DEPFET-System developed with Bonn university



64x64 pixel DEPFET-Matrix JFET type Closed geometry (50x50µm² pixel)

- 64 x 64 matrix with 50 x 50 µm² pixel
- designed for Biomedical Applications
- clock rate : 50 kHz
- achieved noise in matrix: ~50e

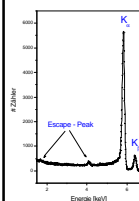
low noise Readout-Chip: CARLOS

G.Lutz, RAL Sept.12, 2003

47

results with prototype system

Single-pixel spectra:



⁵⁵Fe-spectra @ 300K

ENC = 4.8 +/- 0.1 e⁻

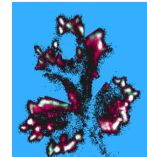
Matrix-picture with ⁵⁵Fe:



~ 3.2 mm

spatial resolution: ~ 9µm (with 50x50 µm² pixel)

Autoradiography with ³H:



~ 10 mm

detection of Tritium ³H (5.6keV mean energy)

[J.Ullrich, Bonn]

G.Lutz, RAL Sept.12, 2003

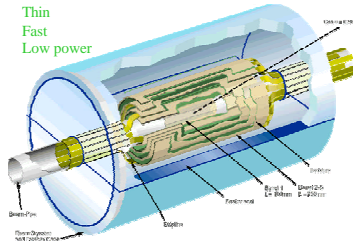
48

Present DEPFET pixel detector development for XEUS and TESLA

In collaboration with Bonn (N.Wermes) and Mannheim (P.Fischer)

TESLA vertex detector

Thin
Fast
Low power



Total > 500 MPixel (with 25x25 μm Pixelsize)
(read out speed 50 MHz)

Options:
CCD
MAPS
HAPS
DEPFET

Layer	Module size	No. of modules
I	25 x 100 mm	1 x 8
II	22 x 125 mm	2 x 8
III	22 x 125 mm	2 x 12
IV	22 x 125 mm	2 x 16
V	22 x 125 mm	2 x 20

G.Lutz, RAL Sept.12, 2003

49

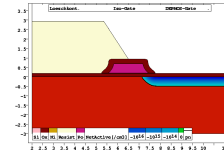
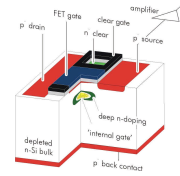
Design of DEPFET pixel detectors

Type of DEPFETS:

MOS-depletion type
XEUS: cylindrical geometry
TESLA: rectangular geometry

Technology:

6 Inch
Double-poly,
double metal,
Self-aligned

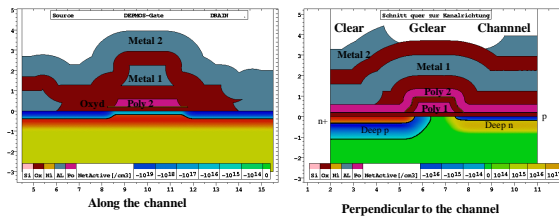


G.Lutz, RAL Sept.12, 2003

50

DEPMOS Technology Simulation

DEPMOS pixel array cuts through one cell



G.Lutz, RAL Sept.12, 2003

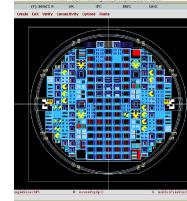
51

Pixel prototype production (6" wafer) for XEUS and LC (TESLA)

Aim: Select design options for an optimized array operation
(no charge loss, high gain, low noise, good clear operation)
On base of these results => production of full size sensors

Many test arrays

- Circular and linear DEPFETS
- up to 128 x 128 pixels
- minimum pixel size about 30 x 30 μm^2
- variety of special test structures



Structures requiring only one metalization layer

Production up to first metal layer finished
Devices are under test
Test results agree very well with device simulations

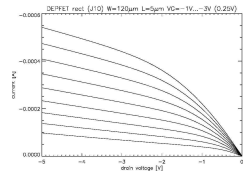
G.Lutz, RAL Sept.12, 2003

52

First DEPFET1 measurements on rectangular test transistors (W = 120 μm L = 5 μm)

Output characteristics:

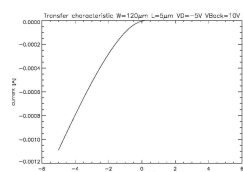
Correct transistor behavior



Transfer characteristics:

Device can be completely switched off

Transistor parameters agree with simulation



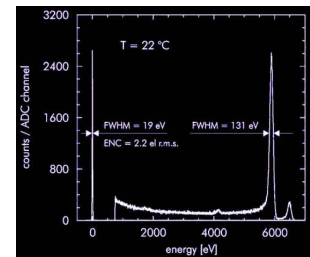
G.Lutz, RAL Sept.12, 2003

53

DEPFET test results: Noise and Spectroscopy

Single circular DEPFET

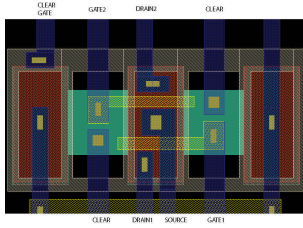
L = 5 μm , W = 40 μm
time-continuous filter, t = 6 μs



G.Lutz, RAL Sept.12, 2003

54

**Rectangular double cell test structure
as used in TESLA pixel prototype**

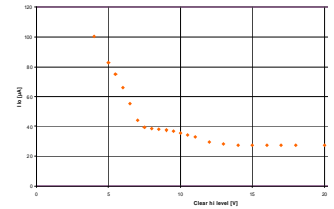


G.Lutz, RAL Sept.12, 2003

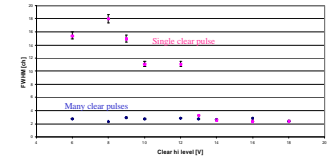
55

**DEPFET test results
Clearing of internal gate:
complete clearing possible?
At which voltage?**

Single rectangular DEPFET:
measure **current** with
cleared internal gate
As function of clear voltage

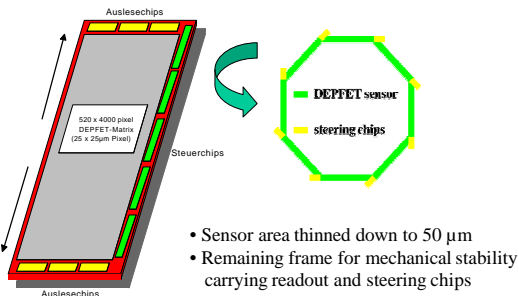


Measure **pedestal noise**
Compare situation of
charge generation followed by
single clear pulse
with
many clear pulses
before reading



56

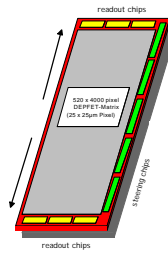
TESLA Module concept with DEPFETs



G.Lutz, RAL Sept.12, 2003

57

Module Concept



5-layer (CCD-like) layout for the vertex detector
1st layer module: sensitive area 100x13 mm²



Estimated Material Budget (1st layer):

Pixel area: 100x13 mm², 50 μm : 0.05% X_0
steer. chips: 100x2 mm², 50 μm : 0.008% X_0
(massive) Frame : 100x4 mm², 300 μm : 0.09% X_0

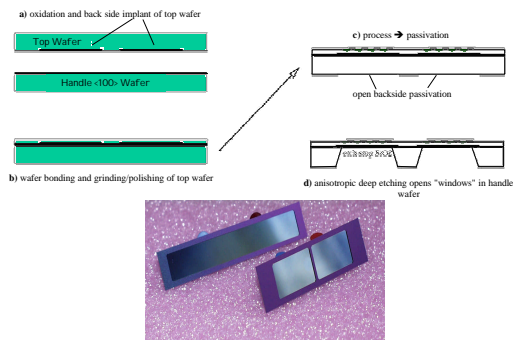
- reduce frame material!!!
by etching of "holes" in the frame
- perforated frame: 0.05% X_0

total: 0.11% X_0

G.Lutz, RAL Sept.12, 2003

58

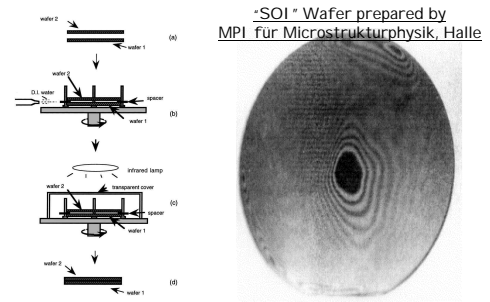
**Processing thin detectors
- the Idea -**



G.Lutz, RAL Sept.12, 2003

59

**Processing thin detectors
- Direct Wafer Bonding -**



O.-Y. Tong and U. Gosele - Semiconductor Wafer Bonding -
John Wiley & Sons, Inc.

picture from: www.mpi-halle.mpg.de
picture from: www.mpi-halle.mpg.de

G.Lutz, RAL Sept.12, 2003

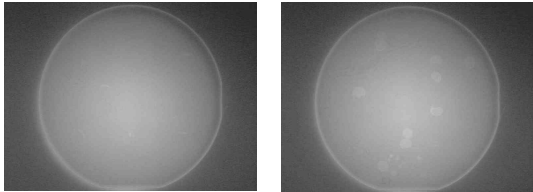
60

Direct Wafer bonding after Implantation

Bonded wafers (structured implant through BOX):

Direct Wafer Bonding possible, but some voids after annealing!

→ improve surface condition before bonding



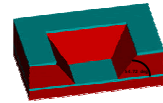
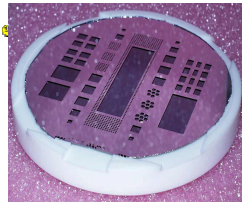
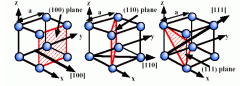
infrared transmission pictures from MPI Halle (M. Reiche)
G.Lutz, RAL Sept.12, 2003

61

Anisotropic Wet Etching - TMAH -

Tetra-Methyl-Ammonium-Hydroxide

good selectivity to oxide
almost perfect selectivity to Al
no alkali ions



G.Lutz, RAL Sept.12, 2003

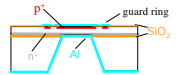
62

Diodes & Teststructures on thin Silicon

* test bondability of implanted oxide & electrical performance of diodes on thin silicon *

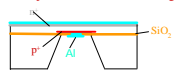
2 types of thinned diodes

Type I: Simplified standard technology



structured p+ on top
unstructured n+ in bond region
3 Wafers

Type II: Implants like DEPFET config.



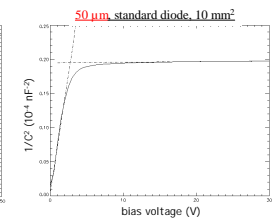
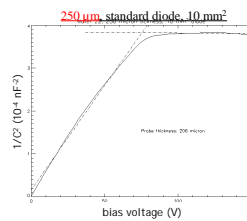
unstructured n+ on top
structured p+ in bond region
3 Wafers

* + 4 Wafers with standard Diodes as a reference *

G.Lutz, RAL Sept.12, 2003

63

Diodes & Teststructures on thin Silicon - Type I: CV curves, full depletion voltage -

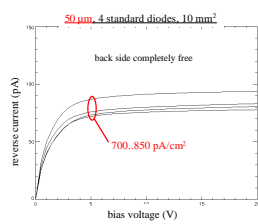
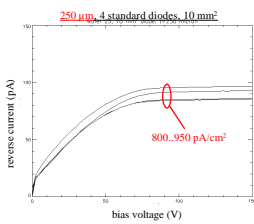


$C(V_{fd}) \rightarrow t = 46 \mu\text{m}$

G.Lutz, RAL Sept.12, 2003

64

Diodes & Teststructures on thin Silicon - Type I: IV curves -

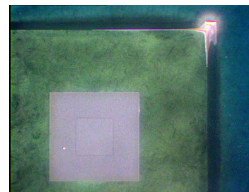


G.Lutz, RAL Sept.12, 2003

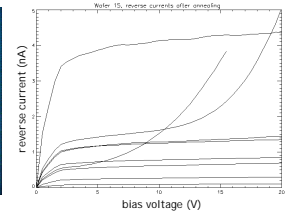
65

Diodes & Teststructures on thin Silicon - Type II: IV curves -

contact opening and metallization
after etching of the handle wafer



Diodes of various sizes: $0.09 \text{ cm}^2 - 6.5 \text{ cm}^2$
- no guard ring -
- surface generated edge current included -
reverse currents after annealing



→ about 2V full depletion voltage
→ about 1 nA/cm² including edge generated current

G.Lutz, RAL Sept.12, 2003

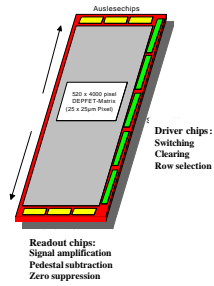
66

Readout electronics for DEPFET pixels

Developed in collaboration with other groups:

- XEUS: MPE, Jülich, Buttler
- TESLA: Bonn, Mannheim, MPI

TESLA readout chip
Current based readout



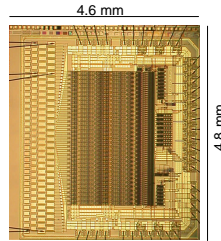
G.Lutz, RAL Sept.12, 2003

67

New steering chip

I.Peric (Bonn), P.Fischer (Mannheim)

Switcher II:

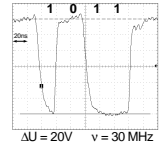


4.8 mm

- AMS 0.8µm HV
- **versatile** sequencing chip (internal sequencer → flexible pattern)
- **high speed + high voltage range** (20V)
- drives 64 DEPFET-rows (can be daisy chained)
- produced 12/2002

Results:

- power consumption: ~1W /channel
- tested ok to 30MHz

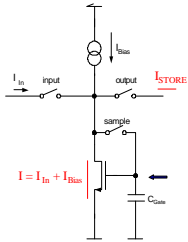


G.Lutz, RAL Sept.12, 2003

68

Current based Readout

How to store a current ??



Storage phase: input and sample-switch closed :
→ gate-capacitance of nmos charged

Sampling phase: input and sample-switch opened :
→ voltage at capacitance „unchanged“
→ **current unchanged**

Transfer phase: output switch closed :
(done immediately after sampling)
→ **I_{STORE} is flowing out**

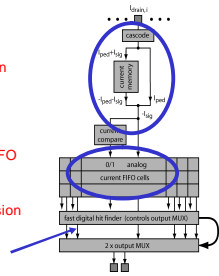
G.Lutz, RAL Sept.12, 2003

69

CURO - Architecture

CURO : **C**urrent **R**ead **O**ut

- front end:
automatic pedestal subtraction (double correlated sampling)
- easy with currents -
- **analog currents buffered in FIFO**
- Hit-Logic performs **0 suppression** and multiplexes hits to ADC (ADC only digitizes hits !)

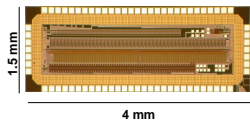


G.Lutz, RAL Sept.12, 2003

70

Results - CURO I (Marcel Trimpl, Bonn)

CURO I:



4 mm

- TSMC 0.25µm, 5metal
- contains all blocks for a fast DEPFET R/O
- radiation tolerant layout rules with annular nmos
- produced 05/2002

digital part:

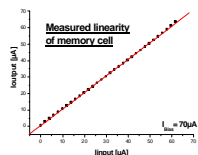
works with desired speed (50MHz)

analog part (current memory cell):

- tested up to: 25MHz
- differential non-linearity: 0.1 %
- noise contribution to readout: < 39nA

Crucial parts of readout work
Design of CURO II submitted
Delivery Dec.03

TESLA Goal:
Thin fullsize pixel matrix 2005



G.Lutz, RAL Sept.12, 2003

71

Summary/Conclusions

Introduction of semiconductor detectors into particle physics (~1980)

- Position (and energy) sensitive
- applications in various fields

Foundation of our laboratory

- with high-tech production technology
- design and test facilities
- dedicated to experiments of two MPIs
 - particle physics
 - X-ray astronomy

- detectors based on new concepts
- developers are also participating in experiments

Present main activities

- DEPFET pixel detectors
- other spectroscopic (drift) detectors

Large development potential

Exciting work lies ahead

G.Lutz, RAL Sept.12, 2003

72